THE JOURNAL OF PHYSICAL CHEMISTRY B

Article

Cite This: J. Phys. Chem. B 2019, 123, 9408−9417

pubs.acs.org/JPCB

Bulk-like and Interfacial Water Dynamics in Nafion Fuel Cell Membranes Investigated with Ultrafast Nonlinear IR Spectroscopy

Sean A. Roget, Patrick L. Kramer,[†] Joseph E. Thomaz, and Michael D. Fayer*

Department of Chemistry, Stanford University, Stanford, California 94305, United States

ABSTRACT: The water confined in the hydrophilic domains of Nafion fuel cell membranes is central to its primary function of ion transport. Water dynamics are intimately linked to proton transfer and are sensitive to the structural features and length scales of confinement. Here, ultrafast polarization-selective pump-probe and two-dimensional infrared vibrational echo (2D IR) experiments were performed on fully hydrated Nafion membranes with sodium counterions to explicate the water dynamics. Like aerosol-OT reverse micelles (AOT RMs), the water dynamics in Nafion are attributed to bulk-like core water in the central region of the hydrophilic domains and much slower interfacial water. Population and orientational dynamics of water in Nafion are slowed by polymer confinement. Comparison of the observed dynamics to those of AOT RMs helps identify local interactions between water and sulfonate anions at the interface and among water molecules in the core. This comparison also demonstrates that the well-known spherical cluster morphology of Nafion is not appropriate. Spectral diffusion of the interfacial water, which arises from structural dynamics, was obtained from the 2D IR experiments taking the core water to have dynamics similar to bulk water. Like the orientational dynamics, spectral diffusion was found to be much slower at the interface compared to bulk water. Together, the dynamics indicate slow reorganization of weakly hydrogen-bonded water molecules at the interface of Nafion. These results provide insights into proton transport mechanisms in fuel cell membranes, and more generally, water dynamics near the interface of confining systems.

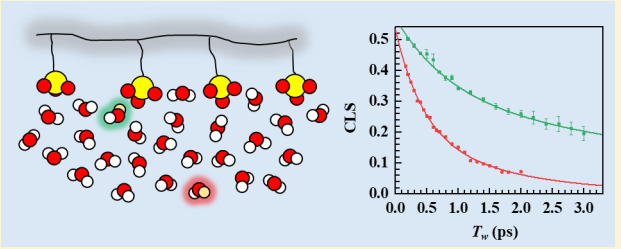

1. INTRODUCTION

Perfluorinated sulfonic acid (PFSA) ionomers have been an active topic of research for many decades, mainly because of their function as ion conducting membranes.[1,2] Nafion was the first PFSA membrane made commercially available and is primarily used for proton exchange in H_2/O_2 fuel cells and sodium ion exchange in electrochemical cells used in the chloroalkali industry. Under harsh chemical conditions, PFSA membranes provide exceptionally high ion conduction and chemical/mechanical durability. A wide range of studies have been done on PFSA polymers by varying the water content, equivalent weight, counterions, and chemical structure of sidechains to find trends in water and ion transport and elucidate polymer morphology to further develop current technologies.[1,2]

PFSA ionomers are random copolymers consisting of a chemically inert, polytetrafluoroethylene backbone and sidechains that are terminated with a sulfonate group. Phase separation of the polymer occurs, due to the contrast between hydrophobic and hydrophilic comonomers, creating an ionic cluster morphology that is further established with hydration. This three-dimensional structure is the key to the ionomer's functional properties and has been studied extensively using small-angle X-ray and neutron scattering.[1−6] However, data from these experiments have been difficult to interpret as the relatively disordered structure results in broad and featureless peaks. Nevertheless, the importance of understanding the polymer structure has led to a number of proposed morphologies. The earliest model, developed by Gierke and Hsu, consisted of spherical clusters, similar to reverse micelles (RMs), (∼4 nm in diameter) that were connected by small channels (∼1 nm in diameter).[3] With years of experimental data for different ionomers under various conditions and improvement of computational simulations, a range of other structural geometries including parallel-cylindrical,[7] lamellar,[8] or less-structured hydrophilic domains confined by locally flat, ribbon-like, or rod-like polymer aggregates[9−11] have been proposed that match the experimental results. Although no conclusive evidence for a precise morphology has been found, the pursuit of defining a structure and understanding how it changes under different conditions continues as this knowledge can guide the design of PFSA polymers to improve ion conductivity and stability.

Proton transport in PFSA membranes has been of major interest, primarily because of its importance in fuel cells. In water, excess protons can diffuse through the medium as a hydronium ion (known as vehicular diffusion) or the excess proton can hop across the water network through a series of making and breaking of hydrogen bonds (H-bonds).[12,13] The latter pathway is called the Grotthuss mechanism, or structural diffusion, and allows protons to diffuse much faster than other ions in water.[14] Simulations have indicated that this

Received: August 8, 2019
Revised: September 30, 2019
Published: October 3, 2019

DOI: 10.1021/acs.jpcb.9b07592
J. Phys. Chem. B 2019, 123, 9408−9417

mechanism is facilitated by particular solvation shell configurations around the excess proton.[15,16] Therefore, the H-bond network rearrangement is important to structural diffusion, and experiments have linked bulk water dynamics to proton transfer.[17,18] In PFSA membranes, proton transport is complicated as the H-bond network is interrupted by the hydrophobic backbone of the polymer and the tethered sulfonate anions. At low water content, it is believed that vehicular diffusion is the only mechanism of proton transport in PFSA membranes but as the water content is increased, proton conductivity is maximized as a more bulk-like H-bond network is established, which allows structural diffusion to play a role in the transport.[19−21] Many reports agree that the core water is the primary contributor to the proton transport in PFSA systems while at the interface, electrostatic interactions between the proton and the sulfonate groups hinder transport.[19,22,23] However, more recent studies have suggested that proton transport at the interface has a significant contribution to proton conductivity.[24,25]

In this report, polarization-selective pump-probe (PSPP) and two-dimensional infrared vibration echo spectroscopies (2D IR) are used to study the dynamics of water confined in fully hydrated Nafion membranes. The protons associated with the sulfonate groups were exchanged for sodium counterions as the presence of the hydronium ion, with its extremely broad absorption features, makes it difficult to observe water dynamics.[26,27] Ultrafast IR spectroscopy has been used to measure H-bond dynamics in bulk water[28−32] as well as aqueous salt solutions,[33,34] polymeric solutions,[35,36] and confining aqueous systems[37−41] to understand water and its interactions in different environments. Experiments on non-bulk systems show that the water dynamics slow in the presence of ions and confining interfaces.

A variety of experimental studies of Nafion reveal that more than one water ensemble exists in the polymer.[25,42,43] Previous steady state and time-resolved IR studies of Nafion, which examined membranes with low to moderate water content, observed two subensembles of water in the linear spectra and population decays.[37,43] The subensembles were identified as water at the core and interface of the hydrophilic domains. These results are similar to aerosol-OT (AOT) RMs, an important model system for studying confined water. For RM diameters of ∼4 nm and larger, the dynamics can be analyzed with a two-component model, consisting of bulk-like water in the core of the RM and a slower population of water interacting with the interface.[38,39] In the previous dynamical study of water in low to moderately hydrated Nafion, time-dependent anisotropy was analyzed without using a two-component model.[37] Thus, core and interfacial water orientational dynamics, which can provide insight into proton transfer in these environments within the membrane, were not determined. Here, a complete two-component analysis of the PSPP experiment of water in fully hydrated Nafion membranes was performed to distinguish the water orientational dynamics of the two subensembles. A comparison to similar studies of AOT RMs was used to identify the water ensemble interactions and to better understand the membrane channel structure and water confinement in Nafion.[39] Furthermore, timescales of complete H-bond network rearrangement at the interface of Nafion were obtained by using a 2D subtraction method to extract 2D IR spectra of the interfacial water. The PSPP and 2D IR experiments were performed on fully hydrated Nafion, which is the standard operating hydration level in fuel cells.[44] Previously, PSPP experiments on Nafion at full hydration and 2D IR experiments were avoided due to issues with scatter (this issue is described in Section 2.1). However, with adequate sample preparation and improvements in data collection, both experiments were performed and the results are reported in this paper. Both dynamical observables in the nonlinear experiments demonstrate that water dynamics are much slower at the interface of the hydrophilic domain than at the core. These dynamics provide insights into the possible proton transport mechanisms at the core and interface of PFSA membranes.

2. EXPERIMENTAL PROCEDURES

2.1. Sample Preparation. Nafion 212 (purchased from fuelcellstore.com) was pretreated by soaking in H_2SO_4 (95−98%, Certified ACS Plus, Fisher Chemical) at 70 °C for 24 h, rinsing with deionized water, and then soaking in H_2O_2 (30%, Certified ACS, Fisher Chemical) at 70 °C for 24 h. This procedure removes possible impurities from the membrane. The membrane was then soaked in 1 M NaCl solution for 24 h to convert it from the acid form ($-SO_3H$) to the sodium form ($-SO_3Na$). Once converted, the membrane was soaked in 6% HOD in H_2O solution for at least 24 h before IR experiments were conducted. The OD stretch of HOD was used as the probe in the IR experiments. HOD has been shown to be an excellent reporter of the molecular dynamics of water (H_2O or D_2O) in various environments. It provides a vibrational local mode rather than the overlapping symmetric and asymmetric stretching modes and can be diluted to minimize resonant energy transfers which can occur in pure water.[29,30,45,46] Membranes were also prepared in H_2O solution rather than the HOD solution to be used for background subtraction of the linear absorption spectrum and to determine the water content. The masses of the membrane fully hydrated and after drying under vacuum for 3 days were recorded. The water content, quantified by $\lambda \equiv n(H_2O)/n(SO_3)$, was determined to be 15.

The samples were sealed between two CaF_2 windows separated by a 150 μm Teflon spacer and filled with paraffin oil. Bulk water samples (6% HOD in H_2O and pure H_2O) were also prepared with a 12 μm Teflon spacer to obtain the linear spectrum and perform 2D IR experiments. The Nafion sample, in the sample cell without oil, scattered laser light, making the signal to noise ratio too low to perform experiments. With oil, there is minimal scattering initially, but it grows on the timescale of hours. This scattering is possibly due to thermal effects seen in Nafion membranes at higher water content including the fully hydrated membranes studied here. The oil provides a medium for thermal contact between the membrane and the windows of the cell. To minimize thermally induced scatter while averaging the data, the sample was moved in increments of 200 μm (a little larger than the diameter of the overlapped IR beams) after every scan (approx 6 min). The oil also ensured that there was no dehydration of the membranes over the course of the nonlinear experiments. Fourier transform infrared (FTIR) spectroscopy was used to confirm that there was no significant change in hydration before and after the experiments.

2.2. Laser System and IR Experiments. Linear IR spectra were measured using a Thermo Scientific Nicolet 6700 FTIR spectrometer (resolution of 1 cm^{-1}) that was purged of atmospheric carbon dioxide and water. 2D IR and PSPP experiments were performed using a laser system and

DOI: 10.1021/acs.jpcb.9b07592
J. Phys. Chem. B 2019, 123, 9408−9417

interferometer previously described in detail.[47] In brief, a Ti:Sapphire oscillator/regenerative amplifier system [2 kHz, 45 fs full width at half-maximum (fwhm), 800 nm output] pumped an optical parametric amplifier system to produce ~60 fs mid-IR pulses centered at 2520 cm^{-1} with a bandwidth of ~230 cm^{-1}. Signals from the nonlinear experiments were spectrally dispersed and detected using a spectrograph which has a 32-pixel mercury cadmium telluride detector. The interferometer was purged with air scrubbed of water and carbon dioxide to minimize any background absorption of the IR pulses and nonlinear signals.

In the PSPP experiment, the IR pulse was split into a strong pump pulse and a weak probe pulse (90:10) and crossed in the sample. The pump was linearly polarized +45° with respect to the probe pulse, which was set to 0° (or horizontally polarized). The time, t, of the probe relative to the pump pulse was scanned using a mechanical delay line. The probe was then resolved immediately after the sample at +45° and −45° to obtain the parallel and perpendicular signals. A final polarizer prior to the monochromator was set at ~0°. This polarizer angle was slightly adjusted to ensure that the two polarizations of the probe beam had exactly the same amplitude on the array detector in the absence of the pump.

In the 2D IR experiment, the mid-IR pulse was split into 4 separate pulses, all horizontally polarized. Three pulses were crossed in the sample, in the box-CARS geometry, to generate a third-order vibrational echo signal in the phase-matched direction. The fourth pulse, or local oscillator (LO), was used for heterodyne detection of the signal. The delay between the first and second pulses, τ, was scanned for a given delay between the second and third pulses, T_w. The ω_τ axis (horizontal) of the 2D spectrum is the initial frequencies of the probe molecules of the chemical system which are labeled by the first two pulses. These frequencies were obtained through a numerical Fourier Transform of the interferogram created by scanning τ. The ω_m axis (vertical) of the 2D spectrum is the final frequencies of the probe molecules after allowing the system to evolve over the period, T_w, and is read out by the third pulse in the sequence that initiates the emission of the echo pulse, which carries the desired information. The ω_m axis was obtained by spectrally resolving the combined echo-LO pulse using the spectrograph. 2D spectra for a range of T_w values were collected to extract the dynamical information from the time (T_w) evolution of the 2D line shape.

3. RESULTS AND DISCUSSION

3.1. Linear IR Spectrum. The background-subtracted and normalized absorption spectrum of the OD stretch of HOD in Nafion (black), which will be referred to as the Nafion spectrum, is shown in Figure 1. The OD stretching mode in water is particularly broad because it is sensitive to the H-bond interactions of the HOD molecule in the H-bond network.[46,48,49] Water ensembles that engage in stronger and/or many H-bonds absorb at lower frequencies while those that engage in weaker and/or fewer H-bonds absorb at higher frequencies. The OD stretch, which is centered at 2509 cm^{-1} and has a fwhm of 160 cm^{-1} in bulk water, is shifted to 2525 cm^{-1} and broadened to 185 cm^{-1} in Nafion. The peak shift and broadening can be attributed to a subensemble of water in Nafion that interacts with the hydrophilic/hydrophobic interface. Moilanen et al. have demonstrated that the Nafion spectrum at different hydration levels can be well separated

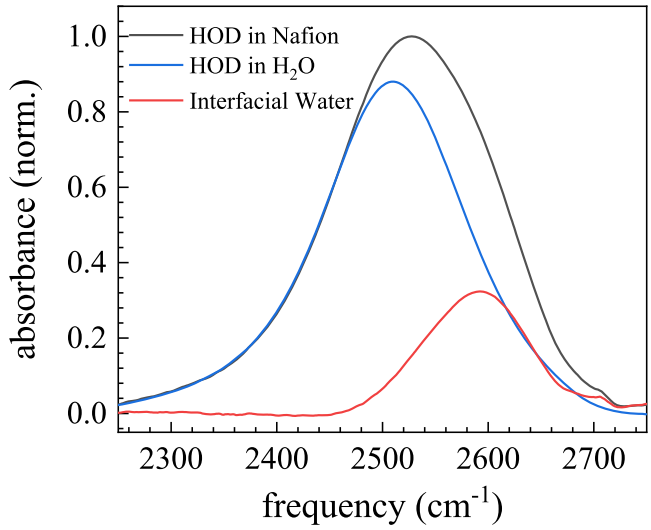

Figure 1. Background subtracted and normalized linear IR spectrum of the OD stretch of HOD in Nafion (black) and its decomposition into its core (blue) and interfacial (red) water spectra.

into a linear combination of the bulk water spectrum and an interfacial water spectrum obtained from a membrane at the lowest hydration measured.[43] Analogous decomposition and similar interfacial water spectra were obtained for AOT RMs.[39] In the Nafion spectrum, there is also a very small peak centered ~2708 cm^{-1}, which is thought to be water embedded in the hydrophobic region of the polymer.

The Nafion spectrum was fit using the bulk water spectrum and an additional Gaussian to represent the interfacial water population. To fit the entire spectrum and obtain the interfacial water spectrum, it is necessary to accurately represent the bulk water spectrum. The spectrum of the OD stretch of HOD in bulk water is asymmetric. It has a large wing on the red side. The wing occurs because the transition dipole of the OD stretch is frequency-dependent. Stronger H-bonding not only causes the absorption to shift to the red but also increases the magnitude of the transition dipole. The frequency-dependent transition dipole is called the non-Condon effect.[50,51] To simplify fitting the Nafion spectrum, the bulk water spectrum was fit with three Gaussians to serve as a simple analytical, but nonphysical, model that very accurately reproduces the bulk water spectrum. In fitting the Nafion spectrum, only the overall amplitude factor of the bulk water model spectrum was allowed to vary. For the additional interfacial water band, the amplitude, center frequency, and fwhm were varied. This procedure provided a constant to appropriately scale the experimental bulk water spectrum so that it can be subtracted from the Nafion spectrum to yield the interfacial water spectrum. The decomposition of the Nafion spectrum is shown in Figure 1. The interfacial water spectrum is centered at 2590 cm^{-1} with fwhm of 114 cm^{-1} which is quite similar to the previously reported spectrum for "dry" Nafion.[43] The interfacial water spectrum is centered at higher frequency than bulk water, indicating that water at the interface, on average, participates in weaker and/or fewer H-bonds. The presence of the interface and the sulfonate groups near it interrupt the H-bond network, resulting in a reduction in the number of H-bonds and the bond strength.

DOI: 10.1021/acs.jpcb.9b07592
J. Phys. Chem. B 2019, 123, 9408−9417

3.2. PSPP Experiment: Population Relaxation. The time dependence of the parallel and perpendicular signals in the PSPP experiments are given by

$$S_{\parallel}(t) = P(t)[1 + 0.8C_2(t)] \quad (1)$$

$$S_{\perp}(t) = P(t)[1 - 0.4C_2(t)] \quad (2)$$

where, $P(t)$ is the population decay of the vibrational mode probed and $C_2(t)$ is the second-order Legendre polynomial orientational correlation function, which reports on the orientational dynamics of the probe molecule. The vibrational relaxation of the OD stretch in water is known to produce a long-lived, isotropic pump-probe signal due to the deposition of energy as heat into the system. This "heating" signal was removed using a well-documented procedure in order to observe the nonlinear signals described by eqs 1 and 2.[28,31] The following linear combination of polarized pump-probe signals

$$P(t) = [S_{\parallel} + 2S_{\perp}]/3 \quad (3)$$

gives the population decay. Because bulk water exists as a single ensemble of molecules interacting through H-bonding with a large homogeneous linewidth and very fast spectral diffusion, the population decay of the OD stretch of HOD in bulk water can be described well by a single exponential fit with a time constant, or lifetime, of 1.8 ps.[31,32]

Representative population decays of the OD stretch of HOD in Nafion (points) are presented in Figure 2. These decays fit

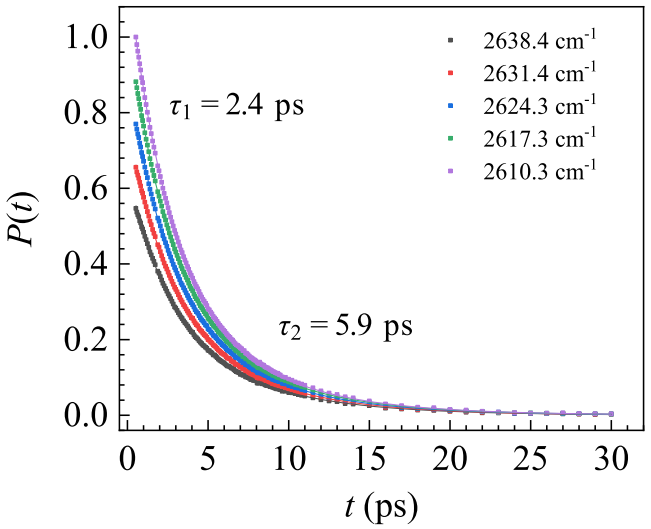

Figure 2. Population decays of the OD stretch of HOD in Nafion from 2610 to 2638 cm^{-1} (points) and the corresponding biexponential fits (curves). All curves are normalized to the value of the 2610.3 cm^{-1} curve at 0.5 ps.

poorly to a single exponential and were best described by biexponential fits shown in Figure 2 (curves). A population decay that is biexponential suggests that there are two ensembles of molecules contributing to the pump-probe signal. In a two-component analysis of the PSPP experiment, the normalized population decay can be expressed as

$$P(t) = aP_1(t) + (1 - a)P_2(t) \quad (4)$$

where, a is the relative amplitude, or contribution, of the first population to the overall population decay and the population decay for each ensemble, $P_i(t)$, is a single exponential. The decomposition of the linear spectrum into bulk and interfacial components provides useful information on how to perform the two-component analysis of the PSPP experiments. Frequencies greater than the center of the interfacial peak were used to avoid contribution from the 1−2 transitions of either population to the signal, which complicates the analysis. The frequency-dependent population decays were fit globally (shown in Figure 2), sharing the two lifetimes and allowing the amplitudes to vary across the frequencies. The lifetimes of the two populations are 2.4 ± 0.1 and 5.9 ± 0.3 ps, respectively, which are slower than the bulk water lifetime of 1.8 ps. A comparison of the lifetimes to those of chemically related systems such as AOT RMs and the relative decays of the 2D line shapes in the 2D IR spectra of water in Nafion (discussed later in Section 3.4), demonstrate that the faster component (2.4 ± 0.1 ps lifetime) is the core population relaxation and the slower component (5.9 ± 0.3 ps lifetime) is the interfacial population relaxation.

In a study of size dependence on the population and orientational dynamics of water in AOT RMs, it was found that large RMs (diameter ≥ ∼6 nm) exhibited two-component dynamics with bulk water dynamics at the center and slow dynamics at the interface. In small RMs (diameter ≤ ∼2.3 nm), much slower dynamics of a single ensemble of water were observed.[39] In between these two ranges, RMs that are ∼4 nm in diameter were identified to be in a "crossover" range, in which the interface affects the dynamics of the core water to some extent. The lifetimes of the two water ensembles in this RM, 2.2 ± 0.1 ps for the core water and 5.3 ± 0.1 ps for the interfacial water, are very close to those observed in Nafion. The lifetime of the OD stretch is very sensitive to the local H-bonding environments of the HOD molecules. It has been observed that water molecules in weak H-bonding configurations, such as water at the interface of RMs or isolated water molecules in ionic liquids,[52,53] have longer lifetimes than in bulk water. The similarity of the lifetimes of the two chemical systems may reflect the similarities of the local environments of the water ensembles. Much like in AOT RMs, the interfacial water of Nafion interacts with sulfonate anions and weakly H-bonded water molecules. The core water molecules, although removed from the interface, are somewhat perturbed by it. The longer lifetime, 2.4 ± 0.1 ps for the core of Nafion versus 1.8 ± 0.1 ps for bulk water, suggests that the H-bonds in the core are slightly weaker than those in bulk water.

The longer lifetime of the core water suggests that the size of the hydrophilic domains in Nafion is in this crossover range where the interface affects all of the water in the Nafion channels to some extent. If the structure of Nafion was composed of spherical clusters proposed by Gierke, by comparison to the results in AOT RMs, the lifetimes suggest that the size of the hydrophilic domains are ∼4 nm, which is in agreement with his estimate.[3] However, the orientational dynamics of water in Nafion discussed below suggest that the domains are not spherical.

3.3. PSPP Experiment: Orientational Relaxation. The orientational dynamics of the probe can be observed through the calculation of the anisotropy given by

$$r(t) = \frac{S_{\parallel}(t) - S_{\perp}(t)}{S_{\parallel}(t) + 2S_{\perp}(t)} = 0.4C_2(t) \quad (5)$$

DOI: 10.1021/acs.jpcb.9b07592
J. Phys. Chem. B 2019, 123, 9408−9417

which, for a single ensemble of probe molecules, provides measurement of the orientational correlation function, $C_2(t)$. This observable, for the HOD probe, tracks the OD bond vector as it undergoes orientational relaxation. Instead of small diffusive steps, water undergoes orientational relaxation via jump reorientation which involves concerted, large-angular motions that occur through breaking and making H-bonds.[54] PSPP experiments on HOD in bulk water have observed that the orientational relaxation through concerted rearrangement of the H-bond network has a time constant of 2.6 ps.[31,32] In aqueous systems, such as concentrated salt solutions, hydrogels, and RMs, reorientation times slow as the H-bond networks are not bulk.

When there are two ensembles of molecules contributing to the pump-probe signal, the anisotropy measures the orientational relaxation of each ensemble weighted by its time-dependent, relative contribution to the population decay.[55] To extract reorientation times, the two-component description of the anisotropy

$$r(t) = 0.4\frac{aP_1(t)C_2^1(t) + (1-a)P_2(t)C_2^2(t)}{aP_1(t) + (1-a)P_2(t)} \quad (6)$$

can be used, where $C_2^i(t)$ is the orientational correlation function for the ith population. This model has been used to assign reorientation times to the core and interfacial ensembles of water and small anion probes in RMs.[39,56] The frequency-dependent relative amplitudes and the lifetime of each ensemble have already been determined from fitting the population decays; thus, the only fitting parameters required by the model are for the orientational correlation functions. In this analysis of the anisotropy of water in Nafion, it is assumed that the correlation functions have the same functional form as bulk water, that is, an ultrafast initial decay due to inertial motions followed by a single exponential decay.[57] The inertial component of the anisotropy decay occurs on a time scale much faster than what can be resolved in PSPP experiments, but it can be characterized by the apparent initial value of the orientational correlation function, that is, the deviation from 0.4 when the anisotropy curve is extrapolated to zero. Thus, four fitting parameters are used to fit the anisotropy decays, where the reorientation time of each ensemble is shared across frequencies.

The anisotropy data (points) and the fits using the two-component model (curves) are shown in Figure 3. The reorientation times for the core and interfacial water subensembles were found to be 2.8 ± 0.2 and 21 ± 3 ps. The fast component, which is associated with the core reorientation, is essentially the same, within experimental error, as that of HOD in bulk water (2.6 ± 0.1 ps).[32] While the core reorientation time is at most slightly slower than that of bulk water, the interfacial reorientation time is considerably slower. In contrast to the population dynamics of Nafion, which resemble 4 nm in diameter RMs, the orientational dynamics are similar to large RMs ≥ ~6 nm in diameter, which have bulk water dynamics at the core and an interfacial reorientation time of 18 ± 3 ps.[39] However, unlike Nafion, HOD in the core of large RMs has the same lifetime as in bulk water. These comparisons are summarized in Table 1.The bulk-like orientational relaxation in the core of Nafion can arise from a difference in the structures of RMs and fully hydrated Nafion. Various morphologies have been used in simulations to reproduce Nafion experimental data, including spherical

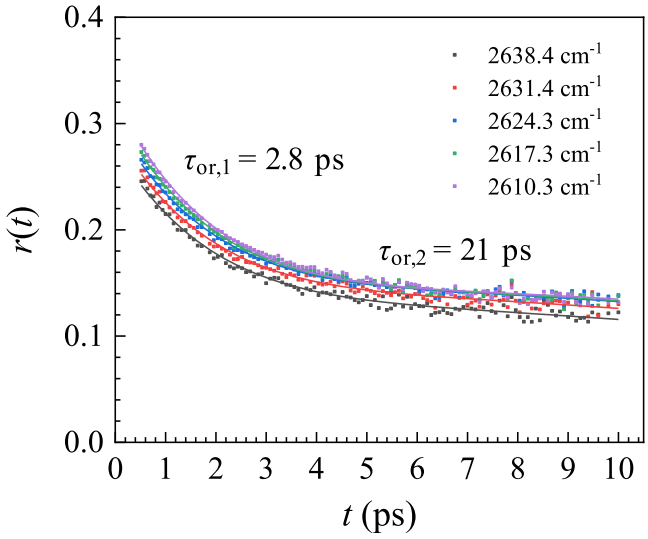

Figure 3. Anisotropy decays of the OD stretch of HOD in Nafion from 2610 to 2638 cm^{-1} (points) and corresponding fits to the two-component model (curves).

Table 1. Summary of Population and Orientational Dynamics of HOD in Nafion, in Two Sizes of RMs and in Bulk Water[a]

system	τ_1 (ps)	τ_2 (ps)	$\tau_{or,1}$ (ps)	$\tau_{or,2}$ (ps)
Nafion	2.4 ± 0.2	5.9 ± 0.3	2.8 ± 0.2	21 ± 3
RM (4 nm)[39]	2.2 ± 0.2	5.3 ± 0.1	4 ± 0.2	26 ± 3
RM (6 nm)[39]	1.8	4.3 ± 0.2	2.6	18 ± 3
bulk water[32]	1.8 ± 0.1		2.6 ± 0.1	

[a] τ_1—lifetime of the core population; τ_2—lifetime of interfacial population; $\tau_{or,1}$—reorientation time of core population; and $\tau_{or,2}$—reorientation time of interfacial population.

clusters[3] and parallel cylindrical channels.[7] Faster orientational dynamics, approaching the bulk time constant, in the core of Nafion would occur if the water molecules existed in a structure with less effective confinement than a spherical cluster. Consider confinement in a sphere versus a cylinder. In a sphere, water is confined in all directions by the interface, whereas, in a cylinder, water is not confined along the longitudinal axis. With reduced confinement, bulk-like orientational dynamics can still occur in a smaller radius cylinder than in a sphere. This is because the orientational relaxation of bulk water is a concerted process involving many water molecules. However, population dynamics are more sensitive to the very local environment, and so these dynamics are still slightly affected by the proximity to the interface.

The largest water pool in the spherical cluster model proposed by Gierke for Nafion with the polymer equivalent weight studied here was 4 nm in diameter.[3] Other suggested models and experimental data report that the hydrophilic domains are much smaller, with diameters of 1−3 nm.[7,11,58] As stated above, the orientational dynamics are the same, within experimental error, as large AOT RMs ≥ 6 nm in diameter. These RM sizes are larger than the range of values reported in the literature for Nafion. The observed Nafion water orientational relaxation is much faster than that observed for RMs in the 1−3 nm range suggested by other models. Moreover, for such small AOT RMs, the surface and core dynamics are not distinct. The reported core orientational

DOI: 10.1021/acs.jpcb.9b07592
J. Phys. Chem. B 2019, 123, 9408−9417

relaxation time for 4 nm AOT RMs is also significantly slower than that measured in Nafion.[39] Thus, the orientational relaxation measurements presented here are not consistent with a spherical cluster model but support a structure which has less severe confinement, such as the model structure of parallel cylindrical channels with an average channel size of 2.4 nm suggested by Schmidt-Rohr and Chen.[7] As discussed above, cylindrical confinement, even with a small cylinder diameter, does not impede orientational relaxation to the same extent as spherical confinement. This is exemplified by experiments and simulation of the orientational dynamics of the selenocyanate anion in water confined in 2.4 nm cylindrical channels of nanoporous silica.[41] In this study, it was found that the orientational dynamics of the selenocyanate anion at the center of the cylindrical channel was essentially the same as that measured in bulk water. These results, and the water dynamics of Nafion observed here, suggest that an average size of 2.4 nm proposed by Chen is reasonable. Parallel cylinders are clearly an idealized model of the Nafion pores. Simulations indicate that the channels have substantial structural inhomogeneity and are not cylindrical on long distance scales.[59] However, on a relatively short distance scale relevant to water/water interactions and dynamics, the morphology is more akin to cylinders than to spheres.

H-bond dynamics, which are required for orientational relaxation of water, are central to the Grotthuss mechanism of proton transport. Jump reorientation is a concerted mechanism in which a water molecule makes a large angular jump. For this to occur, an H-bond is made with an under coordinated water of the second solvation shell and another is broken with an over coordinated first shell water.[54] This process requires the concerted rearrangement of many H-bonds of surrounding water molecules. In a similar manner, simulations indicate that irreversible proton transport occurs by a mechanism where the hydronium ion accepts a fourth H-bond before undergoing proton transport.[15,16] The availability of a water molecule to H-bond to another water molecule (undergoing jump reorientation) or a hydronium ion (undergoing proton transport) depends on the large-scale rearrangement of the H-bond network, which also gives rise to the measured anisotropy decay. Further evidence for this connection was observed in the orientational relaxation of the solvated proton bend in acidic water that was believed to decay due to proton transfer between Zundel-like configurations of the solvated proton.[17] A recent study using 2D IR chemical exchange spectroscopy directly observed proton transfer in concentrated HCl solutions and extrapolated the results to the infinitely dilute limit.[18] The proton transfer hopping time was compared to the slowest component of the spectral diffusion in water measured with 2D IR, and they were found to be identical over a wide temperature range. The slowest component of the spectral diffusion is caused by the H-bond network randomization.[29,30] The conclusion was that the H-bond dynamics that occur in water drive the proton transfer from a hydronium to an H-bonded water molecule. The spectral diffusion measured H-bond network randomization and water orientational relaxation are closely related.

The core reorientation time of HOD in the sodium form of Nafion is the same as in bulk water within error. The protonated form of Nafion used in fuel cell applications can take up more water than the sodium form,[60,61] making the core water even more bulk-like. Experiments have shown that in protonated Nafion, the concentration of hydronium in the core is only 0.5 M.[62] Therefore, the core water is still mostly bulk, and so the nature of proton transfer in the core of protonated Nafion should be essentially the same as in bulk water.

However, proton transport through Nafion channels over macroscopic distances will involve protons experiencing both the core and interfacial environments. The interfacial reorientation time of HOD in Nafion is almost an order of magnitude slower than that in bulk water. Although water/sulfonate H-bonds are weaker than water/water H-bonds, the presence of the interface reduces the pathways available for concerted H-bond rearrangement that is necessary for jump reorientation.[54] The reorientation time of the interfacial water should not be sensitive to higher water content as observed when comparing large RMs of different sizes.[39] Experiments have determined that the proton concentration at the Nafion interface is 1.4 M.[62] (The ratio of the experimental core and interfacial hydronium concentrations[62] are in accord with MD simulations of the free energy difference between the contact ion pair of the sulfonate-hydronium and the solvent separated pair.[63]) The higher proton concentration is due to the attraction of the protons to the interfacial sulfonate groups. At this concentration, most of the water molecules at the interface are not interacting with protons (hydronium cations). Thus, the interfacial reorientational time measured here for the sodium form of Nafion is likely to be very similar in the protonated form of Nafion. Hindered reorientation dynamics can slow proton transfer via structural diffusion (Grotthuss mechanism). The slow orientational relaxation at the interface is in accord with studies that suggest that structural diffusion in the core water is mainly responsible for overall proton conductivity.[19,21,22] If there were to be a significant contribution to proton transport from the interfacial region, the slow reorientation time suggests that the mechanism cannot rely on water H-bond dynamics in the same manner as in bulk water or the core of Nafion. A recent simulation study has suggested that a proton transfer mechanism involving hopping across sulfonates at the surface is the primary mechanism of transport.[24] This study argues against the idea of possible proton trapping due to the electrostatic attraction to the sulfonate anions as it was shown that the first solvation shells of adjacent sulfonate groups overlap.[24] However, if this mechanism requires proton hopping between water molecules in these overlapping solvation shells, the slow reorientation (slow H-bond rearrangement) may be a rate limiting factor.

3.4. 2D IR Experiments. The 2D IR vibrational echo experiment measures spectral diffusion, which is caused by the time-dependent frequency fluctuations of the vibrational mode of the probe molecule due to the structural evolution of its surrounding environment. To quantify the T_w dependence of the 2D IR spectra to yield the spectral diffusion dynamics, the center line slope (CLS) method can be used.[64,65] It has been shown that, for a single ensemble, the CLS(T_w) decay is the normalized frequency−frequency correlation function (FFCF), which is the probability that the vibrational probe with an initial frequency has the same frequency at a later time, averaged over all the frequencies in the inhomogeneously broadened absorption line shape.[64,65] The complete FFCF is typically modeled with the Kubo ansatz:[66,67]

$$\langle \delta\omega(0)\delta\omega(t)\rangle = \sum_i \Delta_i^2 \exp(-t/\tau_i) \tag{7}$$

where, $\delta\omega(t)$ is the instantaneous frequency fluctuation at time, t, while Δ_i and τ_i are the frequency fluctuation amplitude

DOI: 10.1021/acs.jpcb.9b07592
J. Phys. Chem. B 2019, 123, 9408−9417

and time constant of the *i*th decay pathway, respectively. 2D IR experiments and simulations of bulk water have observed a timescale of 0.4 ps that corresponds to local H-bond length fluctuations and a slower timescale of 1.7 ps due to the complete randomization of the H-bond network.[29,30,32] As discussed earlier, the slower timescale has been linked to the proton hopping time in bulk water, suggesting that H-bond rearrangement drives proton transfer in water.[18] Thus, measuring the spectral diffusion of water in Nafion may provide insight into the proton transfer process in the membrane.

Representative 2D IR spectra of HOD in Nafion are presented in Figure 4A. At early T_w, the core water is the major

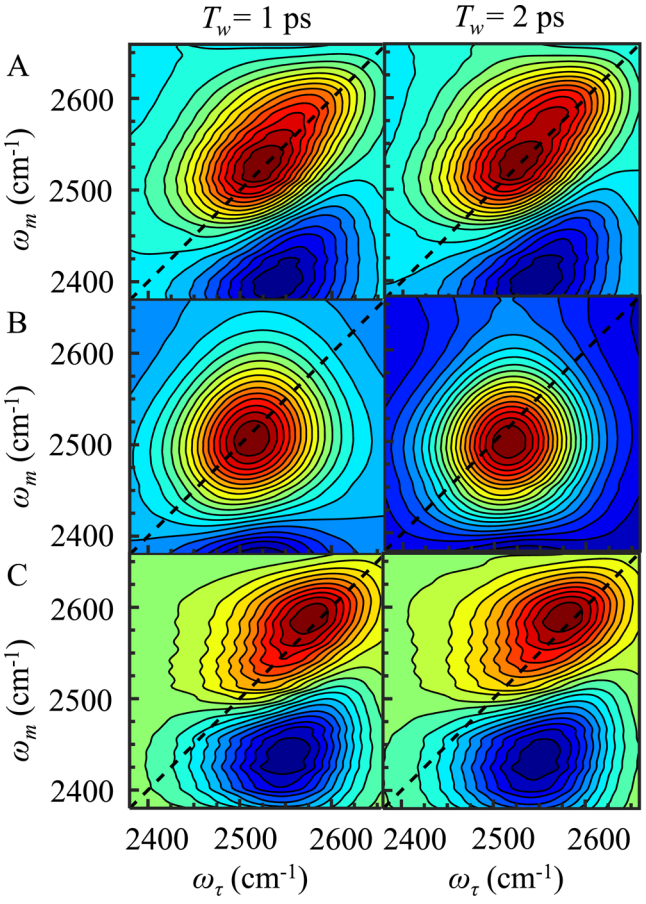

Figure 4. 2D IR spectra at T_ws of 1 and 2 ps of the OD stretch of HOD in (A) Nafion and (B) H_2O. Panel (B) is appropriately scaled and subtracted from (A) to produce (C), the 2D IR spectra of the interfacial water in Nafion at T_ws of 1 and 2 ps.

contributor to the 2D spectrum. However, the interfacial water has a longer lifetime than the core water so the interfacial 2D line shape becomes more apparent at later T_w when the core water signal has decayed. This behavior is in accord with the two-component analyses performed on the linear and PSPP experiments. It has been shown that it is quite difficult to extract spectral diffusion timescales for two-component systems with overlapping 2D line shapes.[68] Here, the spectral diffusion of the water at the interface is of primary interest. The 2D band for the core water is close in frequency to the interfacial band, and so it affects the CLS values of the band of interest.[68] Methods used in past experiments require knowledge of the spectral diffusion dynamics or, equivalently, the 2D line shape of one of the components to extract the CLS values for the unknown component.[68,69] To determine the spectral diffusion of the interfacial water in Nafion, a 2D subtraction method was employed that proved to be successful in observing the dynamics of dihydrogen bonding in sodium borohydride aqueous solutions.[69] In this analysis, the T_w-dependent 2D IR spectra of bulk water (Figure 4B) are scale-subtracted from the 2D IR spectra of water in Nafion (Figure 4A). This assumes that the core water in Nafion has essentially the same 2D line shape at each T_w as bulk water. The fact that the core orientational relaxation is the same as the bulk water orientational relaxation within experimental error supports this assumption.

The linear spectrum decomposition was used to identify a frequency region with little contribution from the interfacial water so that the 2D IR spectrum of bulk water could be accurately scaled to match the core water contribution to the Nafion 2D IR spectrum. Bulk water 2D spectra with the T_ws corresponding to those of the Nafion 2D spectra were used from 0.2 to 2 ps. At longer T_w, it becomes difficult to process the bulk water 2D spectra as the heating signal has a nonnegligible amplitude (the same heating signal mentioned in the PSPP experiment above).[29,30] This is not the case with the Nafion 2D spectrum as the lifetimes of both populations are longer than bulk water, and so the heating signal grows in more slowly and there is a higher ratio of the signal of interest to the heating signal.[28,31] To analyze the Nafion 2D spectra from 2 to 3 ps, the bulk water 2D spectrum at 2 ps was used for subtraction. Most of the bulk water dynamics occur on ultrafast time scales; so by 2 ps, the bulk water spectral diffusion is almost complete. Only 6% of the CLS decay of bulk water, which quantifies the changes in the 2D line shape, occurs over this timescale. In addition, in this time range, the core water contribution to the total 2D spectrum has decayed substantially compared to the interfacial contribution because of its shorter lifetime. This procedure was done over a range of earlier T_ws with a similar change in the CLS value to estimate the error incurred. The mean percentage deviation from the actual CLS value was found to be 5%.

Examples of the results of the subtraction method are shown in Figure 4C. These bands are the 2D IR spectrum of the interfacial water. Some residual amplitude can be seen on the diagonal at 2525 cm^{-1}, which is caused by imperfect subtraction. The CLS data were obtained from the subtracted 2D IR spectra at each T_w. The CLS method only requires a small frequency range about the center of the 2D band of interest; so the residual amplitude around 2525 cm^{-1} has a negligible effect on the frequency range over which the CLS analysis was done. The CLS decays (points) are shown in Figure 5. The CLS data for the bulk water is from the same data set used to subtract the Nafion 2D IR spectrum and is representative of the core water. The CLS decay at the interface was fit to a biexponential (solid curve), giving time constants of 0.9 ± 0.1 and 7 ± 2 ps, which can be compared to the values in bulk water which are 0.4 ± 0.1 and 1.7 ± 0.5 ps.[32] The spectral diffusion dynamics are slower than those observed in bulk water, which indicates that it takes longer to completely sample all of the structures that give rise to the interfacial inhomogeneously broadened absorption line (see Figure 1).

The timescale of the slowest component of the interfacial spectral diffusion is three times faster than the reorientation time. Therefore, the HOD molecules sample the majority of the structural configurations associated with interactions at the

DOI: 10.1021/acs.jpcb.9b07592
J. Phys. Chem. B 2019, 123, 9408−9417

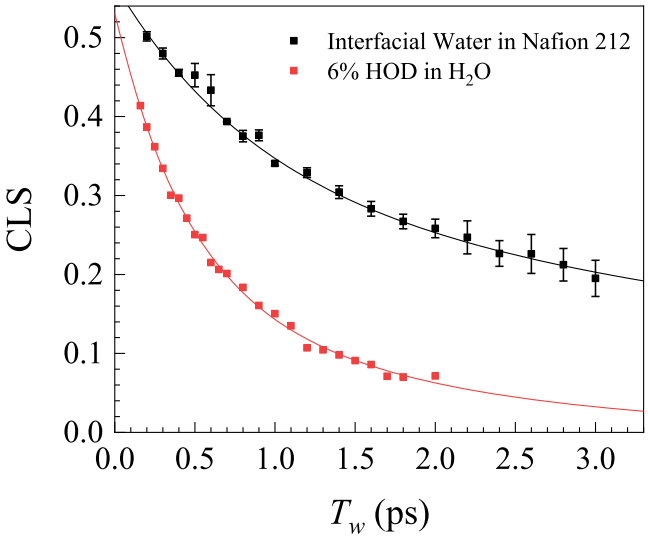

Figure 5. CLS decays (spectral diffusion) of the HOD in H_2O (red points), which is used to model the core water population in Nafion, and the interfacial water (black points), which is obtained as discussed in the text and illustrated in Figure 4. The error bars are the standard error of the CLS values for three experiments. The curves are the biexponential fits.

interface without making large angular jumps. At the Nafion interface, water H-bonds to one of three sulfonate oxygens.[70] These oxygens are not necessarily equivalent due to the local environment. Spectral diffusion could occur through motions of the sulfonate anion and changes in the local environment around the HOD/sulfonate such as motions of other sulfonates and water molecules including those H-bonded to the HOD. Such structural dynamics do not involve large angular changes of the OD bond vector.

It is important to consider how the H-bond dynamics at the interface might affect proton transport in the protonated form of the membrane. If the water ensemble at the interface used the proton transfer mechanism observed in bulk water, the slow orientational relaxation and spectral diffusion timescales suggest that proton transfer is limited at the interface as this H-bond network is not as dynamic as that in the core water.[17,18] However, a hydronium in this water ensemble, with its unique environment of anions and hydrophobic chains, may use a different mechanism for proton transfer such as sulfonate−sulfonate proton hopping.[24] It was mentioned in the discussion of the orientational dynamics that slow water reorientation could be a rate limiting factor in this mechanism due to slow proton transfer across water molecules between adjacent sulfonate groups. However, if the structural fluctuations reflected by the spectral diffusion dynamics drive proton transfer, the time scale would be 7 ps rather than 21 ps orientational relaxation. The results presented here have demonstrated that the core water has properties similar to bulk water, which has a proton hopping time in bulk water of 1.6−1.8 ps.[12,18,71,72] Proton hopping in the core should occur with a hopping time very similar to that in bulk water, which is much faster than the spectral diffusion dynamics at the interface.

4. CONCLUDING REMARKS

In this study, ultrafast PSPP and 2D IR experiments were performed to investigate water dynamics in the sodium form of Nafion 212 at full hydration. A two-component analysis of the population and orientational dynamics from the PSPP experiments was performed to separate the dynamics at the core and interface of the hydrophilic domains of the fully hydrated membrane. The orientational dynamics for these two ensembles have not been determined previously. The observed dynamics were then compared to those of AOT RMs to gain insights into the degree and structure of confinement, and the local interactions of water in Nafion. The population dynamics of water in Nafion were quite similar to those of RMs that are 4 nm in diameter, which display nonbulk dynamics both at the core and the interface of its hydrophilic domain.[39] However, the orientational dynamics of water in Nafion, which had time scales of 2.8 ± 0.2 ps for the core water and 21 ± 3 ps interfacial water, are more similar to those of large AOT RMs.[39] The vibrational lifetime is very sensitive to small changes in H-bond strengths. Population dynamics imply that the water in the core of Nafion is slightly perturbed by the presence of the interface, though the core reorientation is bulk-like. The similarity of the interfacial lifetimes of the OD stretch in Nafion and AOT RMs is due to the similarities of the local interactions in the two systems; specifically, interactions with the sulfonate anions that are present at the interface. The results demonstrate that water in the Nafion core acts essentially like bulk water, and the interfacial water dynamics are the result of interactions with an interface of sulfonate anions. Furthermore, the bulk-like reorientation but perturbed lifetime of the core water in Nafion indicate that the spherical cluster model[3] is not appropriate. Rather a morphology with less restricted confinement, such as the parallel cylinder model,[7] is more suitable.

Spectral diffusion time constants of the interfacial water were obtained using 2D IR spectroscopy. The OD stretch of HOD spectral diffusion at the interface has time constants of 0.9 ± 0.1 and 7 ± 2 ps, which are significantly slower than those in bulk water, 0.4 ± 0.1 and 1.7 ± 0.5 ps.[32] The spectral diffusion time constants arise from structural fluctuations that sample the structural configurations that give rise to the inhomogeneously broadened absorption line. In bulk water, the 0.4 ps time constant is caused by very local OD H-bond fluctuations, mainly the length of the H-bond. The 0.9 ± 0.1 ps time constant in Nafion may also be associated with local OD/sulfonate H-bond fluctuations. In bulk water, the 1.7 ps time constant arises from complete H-bond network randomization,[29,30] which is closely associated with orientational relaxation. At the interface of Nafion, the slow time constant is substantially longer than the corresponding value for bulk water and three times faster than the interfacial orientational relaxation (21 ps). Therefore, the slower dynamics at the Nafion interface are likely associated with structural fluctuations of the sulfonate directly H-bonded to the HOD and the motions of the local sulfonates and water surrounding the HOD vibrational probe.

In bulk water, the time scale for proton hopping via the Grotthuss mechanism is determined by the H-bond rearrangement time observed as the longer time component of the spectral diffusion dynamics.[18] The results presented here indicate that proton transfer in the core of the protonated form of Nafion should be essentially the same as proton transfer in bulk water. Both spectral diffusion and orientational dynamics demonstrate that water interacting with the interface of the hydrophilic domains of Nafion undergo considerably slower dynamics than in the bulk-like core of Nafion. The fast

DOI: 10.1021/acs.jpcb.9b07592
J. Phys. Chem. B 2019, 123, 9408−9417

dynamics of the core water and slow dynamics of the interfacial water is largely in agreement with the idea that the majority of the proton conductivity occurs in the core. However, a proton transfer mechanism unique to the interface has been proposed that places much of proton transfer at the interface.[24] Further ultrafast IR experiments can be performed on PFSA polymers with various side-chains to better understand how the interfacial structure affects the water dynamics. Correlating the water dynamics of several PFSA polymers with overall conductivity may provide an answer to whether the proton transport is more important at the core or the interface of the hydrophilic domains and could provide insights for the development of improved membranes. In addition, recent 2D IR chemical exchange spectroscopy in bulk water/HCl solutions, which directly observed proton hopping, can be extended to Nafion and other PFSA polymers.[18] Using the dynamical information found in this study as observables for simulations could provide additional insights into water dynamics, proton transfer mechanisms and how water dynamics are related to proton transfer in PFSA ionomers.

AUTHOR INFORMATION

Corresponding Author

*E-mail: fayer@stanford.edu. Phone: (650) 723-4446.

ORCID

Michael D. Fayer: 0000-0002-0021-1815

Present Address

†Linac Coherent Light Source, SLAC National Accelerator Laboratory, Menlo Park, CA 94025, United States.

Notes

The authors declare no competing financial interest.

ACKNOWLEDGMENTS

This work was supported by the Division of Chemical Sciences, Geosciences, and Biosciences, Office of Basic Energy Sciences of the U.S. Department of Energy through grant no. DEFG03-84ER13251. J.E.T. thanks the National Science Foundation for a graduate fellowship and P.L.K. thanks the ARCS Foundation for partial financial support through an ARCS fellowship. S.A.R. also thanks Steven A. Yamada for many stimulating discussions.

REFERENCES

(1) Mauritz, K. A.; Moore, R. B. State of Understanding of Nafion. *Chem. Rev.* **2004**, *104*, 4535−4586.

(2) Kusoglu, A.; Weber, A. Z. New Insights into Perfluorinated Sulfonic-Acid Ionomers. *Chem. Rev.* **2017**, *117*, 987−1104.

(3) Hsu, W. Y.; Gierke, T. D. Ion Transport and Clustering in Nafion Perfluorinated Membranes. *J. Membr. Sci.* **1983**, *13*, 307−326.

(4) Gebel, G.; Diat, O. Neutron and X-Ray Scattering: Suitable Tools for Studying Ionomer Membranes. *Fuel Cells* **2005**, *5*, 261−276.

(5) Kim, M.-H.; Glinka, C. J.; Grot, S. A.; Grot, W. G. SANS Study of the Effects of Water Vapor Sorption on the Nanoscale Structure of Perfluorinated Sulfonic Acid (Nafion) Membranes. *Macromolecules* **2006**, *39*, 4775−4787.

(6) Elliott, J. A.; Wu, D.; Paddison, S. J.; Moore, R. B. A Unified Morphological Description of Nafion Membranes from SAXS and Mesoscale Simulations. *Soft Matter* **2011**, *7*, 6820−6827.

(7) Schmidt-Rohr, K.; Chen, Q. Parallel Cylindrical Water Nanochannels in Nafion Fuel-Cell Membranes. *Nat. Mat.* **2008**, *7*, 75−83.

(8) Litt, M. A. Reevaluation of Nafion(R) Morphology. *Abstr. Pap. Am. Chem. Soc.* **1997**, *213*, 33.

(9) Rollet, A.-L.; Diat, O.; Gebel, G. A New Insight into Nafion Structure. *J. Phys. Chem. B* **2002**, *106*, 3033−3036.

(10) Rubatat, L.; Rollet, A. L.; Gebel, G.; Diat, O. Evidence of Elongated Polymeric Aggregates in Nafion. *Macromolecules* **2002**, *35*, 4050−4055.

(11) Kreuer, K.-D.; Portale, G. A Critical Revision of the Nano-Morphology of Proton Conducting Ionomers and Polyelectrolytes for Fuel Cell Applications. *Adv. Funct. Mater.* **2013**, *23*, 5390−5397.

(12) Agmon, N. The Grotthuss Mechanism. *Chem. Phys. Lett.* **1995**, *244*, 456−462.

(13) Marx, D. Proton Transfer 200 Years after Von Grotthuss: Insights from Ab Initio Simulations. *ChemPhysChem* **2006**, *7*, 1848−1870.

(14) Roberts, N. K.; Northey, H. L. Proton and Deuteron Mobility in Normal and Heavy Water Solutions of Electrolytes. *J. Chem. Soc., Faraday Trans. 1* **1974**, *70*, 253−262.

(15) Berkelbach, T. C.; Lee, H.-S.; Tuckerman, M. E. Concerted Hydrogen-Bond Dynamics in the Transport Mechanism of the Hydrated Proton: A First-Principles Molecular Dynamics Study. *Phys. Rev. Lett.* **2009**, *103*, 238302.

(16) Biswas, R.; Tse, Y.-L. S.; Tokmakoff, A.; Voth, G. A. Role of Presolvation and Anharmonicity in Aqueous Phase Hydrated Proton Solvation and Transport. *J. Phys. Chem. B* **2016**, *120*, 1793−1804.

(17) Carpenter, W. B.; Fournier, J. A.; Lewis, N. H. C.; Tokmakoff, A. Picosecond Proton Transfer Kinetics in Water Revealed with Ultrafast IR Spectroscopy. *J. Phys. Chem. B* **2018**, *122*, 2792−2802.

(18) Yuan, R.; Napoli, J. A.; Yan, C.; Marsalek, O.; Markland, T. E.; Fayer, M. D. Tracking Aqueous Proton Transfer by Two-Dimensional Infrared Spectroscopy and Ab Initio Molecular Dynamics Simulations. *ACS Cent. Sci.* **2019**, *5*, 1269.

(19) Paddison, S. J.; Paul, R. The nature of proton transport in fully hydrated Nafion. *Phys. Chem. Chem. Phys.* **2002**, *4*, 1158−1163.

(20) Cui, S.; Liu, J.; Selvan, M. E.; Keffer, D. J.; Edwards, B. J.; Steele, W. V. A Molecular Dynamics Study of a Nafion Polyelectrolyte Membrane and the Aqueous Phase Structure for Proton Transport. *J. Phys. Chem. B* **2007**, *111*, 2208−2218.

(21) Kreuer, K. D.; Schuster, M.; Obliers, B.; Diat, O.; Traub, U.; Fuchs, A.; Klock, U.; Paddison, S. J.; Maier, J. Short-Side-Chain Proton Conducting Perfluorosulfonic Acid Ionomers: Why They Perform Better in PEM Fuel Cells. *J. Power Sources* **2008**, *178*, 499−509.

(22) Choi, P.; Jalani, N. H.; Datta, R. Thermodynamics and Proton Transport in Nafion. *J. Electrochem. Soc.* **2005**, *152*, A1548.

(23) Karo, J.; Aabloo, A.; Thomas, J. O.; Brandell, D. Molecular Dynamics Modeling of Proton Transport in Nafion and Hyflon Nanostructures. *J. Phys. Chem. B* **2010**, *114*, 6056−6064.

(24) Savage, J.; Tse, Y.-L. S.; Voth, G. A. Proton Transport Mechanism of Perfluorosulfonic Acid Membranes. *J. Phys. Chem. C* **2014**, *118*, 17436−17445.

(25) Ling, X.; Bonn, M.; Domke, K. F.; Parekh, S. H. Correlated Interfacial Water Transport and Proton Conductivity in Perfluorosulfonic Acid Membranes. *Proc. Natl. Acad. Sci. U.S.A.* **2019**, *116*, 8715.

(26) Napoli, J. A.; Marsalek, O.; Markland, T. E. Decoding the Spectroscopic Features and Time Scales of Aqueous Proton Defects. *J. Chem. Phys.* **2018**, *148*, 222833.

(27) Fournier, J. A.; Carpenter, W. B.; Lewis, N. H. C.; Tokmakoff, A. Broadband 2D IR Spectroscopy Reveals Dominant Asymmetric $H_5O_2^+$ Proton Hydration Structures in Acid Solutions. *Nat. Chem.* **2018**, *10*, 932−937.

(28) Steinel, T.; Asbury, J. B.; Zheng, J.; Fayer, M. D. Watching Hydrogen Bonds Break: A Transient Absorption Study of Water. *J. Phys. Chem. A* **2004**, *108*, 10957−10964.

(29) Asbury, J. B.; Steinel, T.; Kwak, K.; Corcelli, S. A.; Lawrence, C. P.; Skinner, J. L.; Fayer, M. D. Dynamics of Water Probed with Vibrational Echo Correlation Spectroscopy. *J. Chem. Phys.* **2004**, *121*, 12431−12446.

(30) Asbury, J. B.; Steinel, T.; Stromberg, C.; Corcelli, S. A.; Lawrence, C. P.; Skinner, J. L.; Fayer, M. D. Water Dynamics:

DOI: 10.1021/acs.jpcb.9b07592
J. Phys. Chem. B 2019, 123, 9408−9417

Vibrational Echo Correlation Spectroscopy and Comparison to Molecular Dynamics Simulations. *J. Phys. Chem. A* **2004**, *108*, 1107−1119.
(31) Rezus, Y. L. A.; Bakker, H. J. On the Orientational Relaxation of HDO in Liquid Water. *J. Chem. Phys.* **2005**, *123*, 114502.
(32) Park, S.; Fayer, M. D. Hydrogen Bond Dynamics in Aqueous NaBr Solutions. *Proc. Natl. Acad. Sci. U.S.A.* **2007**, *104*, 16731.
(33) Giammanco, C. H.; Wong, D. B.; Fayer, M. D. Water Dynamics in Divalent and Monovalent Concentrated Salt Solutions. *J. Phys. Chem. B* **2012**, *116*, 13781−13792.
(34) Bakker, H. J. Structural Dynamics of Aqueous Salt Solutions. *Chem. Rev.* **2008**, *108*, 1456−1473.
(35) Verma, P. K.; Kundu, A.; Ha, J.-H.; Cho, M. Water Dynamics in Cytoplasm-Like Crowded Environment Correlates with the Conformational Transition of the Macromolecular Crowder. *J. Am. Chem. Soc.* **2016**, *138*, 16081−16088.
(36) Yan, C.; Kramer, P. L.; Yuan, R.; Fayer, M. D. Water Dynamics in Polyacrylamide Hydrogels. *J. Am. Chem. Soc.* **2018**, *140*, 9466−9477.
(37) Moilanen, D. E.; Piletic, I. R.; Fayer, M. D. Water Dynamics in Nafion Fuel Cell Membranes: The Effects of Confinement and Structural Changes on the Hydrogen Bond Network. *J. Phys. Chem. C* **2007**, *111*, 8884−8891.
(38) Moilanen, D. E.; Fenn, E. E.; Wong, D.; Fayer, M. D. Water Dynamics at the Interface in AOT Reverse Micelles. *J. Phys. Chem. B* **2009**, *113*, 8560−8568.
(39) Moilanen, D. E.; Fenn, E. E.; Wong, D.; Fayer, M. D. Water Dynamics in Large and Small Reverse Micelles: From Two Ensembles to Collective Behavior. *J. Chem. Phys.* **2009**, *131*, 014704.
(40) Moilanen, D. E.; Fenn, E. E.; Wong, D.; Fayer, M. D. Geometry and Nanolength Scales Versus Interface Interactions: Water Dynamics in AOT Lamellar Structures and Reverse Micelles. *J. Am. Chem. Soc.* **2009**, *131*, 8318−8328.
(41) Yamada, S. A.; Shin, J. Y.; Thompson, W. H.; Fayer, M. D. Water Dynamics in Nanoporous Silica: Ultrafast Vibrational Spectroscopy and Molecular Dynamics Simulations. *J. Phys. Chem. C* **2019**, *123*, 5790−5803.
(42) Falk, M. An Infrared Study of Water in Perfluorosulfonate (Nafion) Membranes. *Can. J. Chem.* **1980**, *58*, 1495−1501.
(43) Moilanen, D. E.; Piletic, I. R.; Fayer, M. D. Tracking Water's Response to Structural Changes in Nafion Membranes. *J. Phys. Chem. A* **2006**, *110*, 9084−9088.
(44) Hussey, D. S.; Spernjak, D.; Weber, A. Z.; Mukundan, R.; Fairweather, J.; Brosha, E. L.; Davey, J.; Spendelow, J. S.; Jacobson, D. L.; Borup, R. L. Accurate Measurement of the through-Plane Water Content of Proton-Exchange Membranes Using Neutron Radiography. *J. Appl. Phys.* **2012**, *112*, 104906.
(45) Woutersen, S.; Bakker, H. J. Resonant Intermolecular Transfer of Vibrational Energy in Liquid Water. *Nature* **1999**, *402*, 507−509.
(46) Corcelli, S. A.; Lawrence, C. P.; Skinner, J. L. Combined Electronic Structure/Molecular Dynamics Approach for Ultrafast Infrared Spectroscopy of Dilute HOD in Liquid H2O and D2O. *J. Chem. Phys.* **2004**, *120*, 8107−8117.
(47) Fenn, E. E.; Wong, D. B.; Fayer, M. D. Water Dynamics in Small Reverse Micelles in Two Solvents: Two-Dimensional Infrared Vibrational Echoes with Two-Dimensional Background Subtraction. *J. Chem. Phys.* **2011**, *134*, 054512.
(48) Lawrence, C. P.; Skinner, J. L. Vibrational Spectroscopy of HOD in Liquid D2O. III. Spectral Diffusion, and Hydrogen-Bonding and Rotational Dynamics. *J. Chem. Phys.* **2002**, *118*, 264−272.
(49) Corcelli, S. A.; Skinner, J. L. Infrared and Raman Line Shapes of Dilute HOD in Liquid H2O and D2O from 10 to 90 °C. *J. Phys. Chem. A* **2005**, *109*, 6154−6165.
(50) Schmidt, J. R.; Corcelli, S. A.; Skinner, J. L. Pronounced Non-Condon Effects in the Ultrafast Infrared Spectroscopy of Water. *J. Chem. Phys.* **2005**, *123*, 044513.
(51) Schmidt, J. R.; Roberts, S. T.; Loparo, J. J.; Tokmakoff, A.; Fayer, M. D.; Skinner, J. L. Are Water Simulation Models Consistent with Steady-State and Ultrafast Vibrational Spectroscopy Experiments? *Chem. Phys.* **2007**, *341*, 143−157.
(52) Wong, D. B.; Giammanco, C. H.; Fenn, E. E.; Fayer, M. D. Dynamics of Isolated Water Molecules in a Sea of Ions in a Room Temperature Ionic Liquid. *J. Phys. Chem. B* **2013**, *117*, 623−635.
(53) Kramer, P. L.; Giammanco, C. H.; Fayer, M. D. Dynamics of Water, Methanol, and Ethanol in a Room Temperature Ionic Liquid. *J. Chem. Phys.* **2015**, *142*, 212408.
(54) Laage, D.; Hynes, J. T. A Molecular Jump Mechanism of Water Reorientation. *Science* **2006**, *311*, 832−835.
(55) Piletic, I. R.; Moilanen, D. E.; Spry, D. B.; Levinger, N. E.; Fayer, M. D. Testing the Core/Shell Model of Nanoconfined Water in Reverse Micelles Using Linear and Nonlinear IR Spectroscopy. *J. Phys. Chem. A* **2006**, *110*, 4985−4999.
(56) Yuan, R.; Yan, C.; Nishida, J.; Fayer, M. D. Dynamics in a Water Interfacial Boundary Layer Investigated with IR Polarization-Selective Pump−Probe Experiments. *J. Phys. Chem. B* **2017**, *121*, 4530−4537.
(57) Moilanen, D. E.; Fenn, E. E.; Lin, Y.-S.; Skinner, J. L.; Bagchi, B.; Fayer, M. D. Water Inertial Reorientation: Hydrogen Bond Strength and the Angular Potential. *Proc. Natl. Acad. Sci. U.S.A.* **2008**, *105*, 5295.
(58) Duan, Q.; Wang, H.; Benziger, J. Transport of Liquid Water through Nafion Membranes. *J. Membr. Sci.* **2012**, *392*−*393*, 88−94.
(59) Knox, C. K.; Voth, G. A. Probing Selected Morphological Models of Hydrated Nafion Using Large-Scale Molecular Dynamics Simulations. *J. Phys. Chem. B* **2010**, *114*, 3205−3218.
(60) Jalani, N. H.; Datta, R. The effect of equivalent weight, temperature, cationic forms, sorbates, and nanoinorganic additives on the sorption behavior of Nafion. *J. Membr. Sci.* **2005**, *264*, 167−175.
(61) Shi, S.; Weber, A. Z.; Kusoglu, A. Structure-Transport Relationship of Perfluorosulfonic-Acid Membranes in Different Cationic Forms. *Electrochim. Acta* **2016**, *220*, 517−528.
(62) Spry, D. B.; Fayer, M. D. Proton Transfer and Proton Concentrations in Protonated Nafion Fuel Cell Membranes. *J. Phys. Chem. B* **2009**, *113*, 10210−10221.
(63) Petersen, M. K.; Voth, G. A. Characterization of the Solvation and Transport of the Hydrated Proton in the Perfluorosulfonic Acid Membrane Nafion. *J. Phys. Chem. B* **2006**, *110*, 18594−18600.
(64) Kwak, K.; Park, S.; Finkelstein, I. J.; Fayer, M. D. Frequency-Frequency Correlation Functions and Apodization in Two-Dimensional Infrared Vibrational Echo Spectroscopy: A New Approach. *J. Chem. Phys.* **2007**, *127*, 124503.
(65) Kwak, K.; Rosenfeld, D. E.; Fayer, M. D. Taking Apart the Two-Dimensional Infrared Vibrational Echo Spectra: More Information and Elimination of Distortions. *J. Chem. Phys.* **2008**, *128*, 204505.
(66) Hamm, P.; Zanni, M. *Concepts and Methods of 2D Infrared Spectroscopy*; Cambridge University Press: New York, 2011.
(67) Kubo, R. In *Fluctuation, Relaxation, and Resonance in Magnetic Systems*; Haar, D. T., Ed.; Oliver and Boyd: London, 1962.
(68) Fenn, E. E.; Fayer, M. D. Extracting 2D IR Frequency-Frequency Correlation Functions from Two Component Systems. *J. Chem. Phys.* **2011**, *135*, 074502.
(69) Giammanco, C. H.; Kramer, P. L.; Fayer, M. D. Dynamics of Dihydrogen Bonding in Aqueous Solutions of Sodium Borohydride. *J. Phys. Chem. B* **2015**, *119*, 3546−3559.
(70) Petersen, M. K.; Voth, G. A. Characterization of the Solvation and Transport of the Hydrated Proton in the Perfluorosulfonic Acid Membrane Nafion. *J. Phys. Chem. B* **2006**, *110*, 18594−18600.
(71) Meiboom, S. Nuclear Magnetic Resonance Study of the Proton Transfer in Water. *J. Chem. Phys.* **1961**, *34*, 375−388.
(72) Light, T. S.; Licht, S.; Bevilacqua, A. C.; Morash, K. R. The Fundamental Conductivity and Resistivity of Water. *Electrochem. Solid-State Lett.* **2005**, *8*, E16−E19.

DOI: 10.1021/acs.jpcb.9b07592
J. Phys. Chem. B 2019, 123, 9408−9417